[10] J. D. Kraus, *Antennas,* 2nd ed. New York: McGraw-Hill, 1988, pp. 175–188.
[11] *IEEE Standard Test Procedures for Antennas, ANSI/IEEE Std. 149-179.* New York: IEEE and Wiley-Interscience, 1979, pp. 110–112.
[12] C. Chi and G. M. Rebeiz, "A Quasioptical amplifier," *IEEE Microwave Guided Wave Lett.,* vol. 3, no. 6, pp. 164–166, 1993.
[13] M. Kim, J. J. Rosenberg, R. P. Smith, R. M. Weikle, II, J. B. Hacker, M. P. DeLisio, and D. B. Rutledge, "A grid amplifier," *IEEE Microwave Guided Wave Lett.,* vol. 1, no. 11, pp. 322–324, 1991.
[14] T. P. Budka, M. W. Trippe, S. Weinreb, and G. M. Rebeiz, "A 75–115 GHz quasioptical amplifier," *IEEE Trans. Microwave Theory Tech.*, vol. MTT-42, no. 5, pp. 899–901, 1994.
[15] N. Sheth, T. Ivanov, A. Balasubramaniyan, and A. Mortazawi, "A nine HEMT spatial amplifier," in *1994 IEEE MTT-S Int. Microwave Symp. Dig.,* San Diego, CA, May 1994, vol. 2, pp. 1239–1242.
[16] D. R. Gagnon, "Lens-focused measurements for quasioptical components," in *Workshop Notes for Circuit Level Designing and Modeling of Quasioptical Circuits and Systems at the 1994 Int. Microwave Symp.,* San Diego, CA, June 1994; and D. R. Gagnon, "Highly sensitive measurements with a lens-focused reflectometer," *IEEE Trans. Microwave Theory Tech.,* vol. 39, pp. 2237–2240, Dec. 1991.
[17] M. Kim *et al.,* "A 100-element HBT grid amplifier," *IEEE Trans. Microwave Theory Tech.,* vol. 41, no. 10, pp. 1762–1771, 1993.
[18] D. Rutledge *et al.,* "Oscillator and amplifier grids," in *IEEE Int. Microwave Symp. Dig.,* Albuquerque, NM, June 1992, vol. 1, pp. 815–818.
[19] H. J. Kuno, "Analysis of nonlinear characteristics and transient response of IMPATT amplifiers," *IEEE Trans. Microwave Theory Tech.,* vol. MTT-21, no. 11, pp. 694–702, 1973.
[20] L. J. Kushner, "Output performance of idealized microwave power amplifiers," *Microwave J.,* vol. 32, no. 10, pp. 103–116, 1989.

General Formulas for the Method of Lines in Cylindrical Coordinates

Reinhold Pregla

***Abstract*— General formulas are given for the method of lines in cylindrical coordinates and angular discretization. They describe the transfer of the fields from one boundary of a cylindrical layer to another in a multilayered structure. With these formulas, programming can be accomplished without performing additional analysis.**

I. Introduction

The method of lines, as a special FDM, enables analytic calculation in a specific direction. In this direction, the structures to be analysed can consist of multiple, stacked layers without causing an increase in the difficulty or complexity of the analysis. In general, field components from the boundary surface of one layer can be transformed to that of another layer. The basic theory and important formulas for this procedure are explained in [1]. These transformation formulas are easily suited to the analysis of waveguides such as those used in integrated optics, [2], [3] and diffused waveguides with up to 80 layers or more can be modeled using this method.

Of late, cylindrical structures have also become more meaningful. The basic principle of using the method of lines to solve wave equations in cylindrical coordinates is given in [4]. A treatment of microstrip lines of arbitrary cross section, accomplished with the help of cylindrical functions, appears in [5], and in [6] the analysis of antennas composed of microstrip and microslot resonators using cylindrical bodies is explained. Dipoles are analyzed in [7] using the methodology described in [1]. A generalized description of the transformation of fields from one cylindrical boundary surface to another, however, has not been completed. The purpose of this document is to provide such a description. Having such general formulas computer programming is made very easy.

Manuscript received October 3, 1994; revised December 31, 1994.
The author is with Fern Universitaet in D-58084 Hagen, Germany.
IEEE Log Number 9412057.

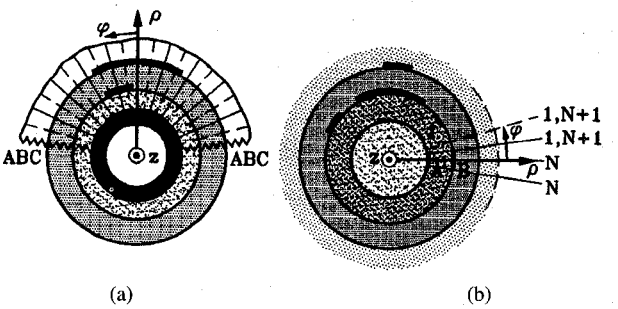

Fig. 1. Cross sections of cylindrical multilayer structures with discretization lines using ABC's (a) and PBC'c (b). (a) General cross section, (b) sectorial cross section.

II. Methods of Analysis

The general method of analysis, described below, applies to structures such as those diagrammed in Fig. 1. The number of layers in these structures is arbitrary. An arbitrary number of metallic strips or cylinders can be placed between the layers of the structure, and the layers can begin at $\rho = 0$ and extend to infinity. Structures with a ρ-dependent permittivity (graded index fibers) can be successfully modeled by a sufficient number of distinct layers. The goal of this document is thus the formulation of a general transfer for fields between two boundary layers, i.e. from a surface A to a surface B in the ith layer. The procedure for this is analogous to those in [1] and [8], [9], but in cylindrical coordinates and with angular discretization. The permittivities in the layers can also be complex.

The whole field may be obtained from the components in the z direction, e_z and h_z. These are the only Cartesian components in the cylindrical coordinate system, and for these components the following wave equations are valid

$$\overline{\nabla}_t^2 F_z + \frac{\partial^2 F_z}{\partial \overline{z}^2} + \varepsilon_r F_z = 0 \tag{1}$$

where $F_z = E_z$ or $F_z = \tilde{H}_z = \eta_o H_z, \overline{z} = k_o z, \overline{\rho} = k_o \rho$ and

$$\overline{\nabla}_t^2 = \frac{1}{\overline{\rho}} \frac{\partial}{\partial \overline{\rho}} \left(\overline{\rho} \frac{\partial}{\partial \overline{\rho}} \right) + \frac{1}{\overline{\rho}^2} \frac{\partial^2}{\partial \varphi^2} \tag{2}$$

is the Laplace operator in cylindrical coordinates.k_o and η_o are the wave number and wave impedance of free space, respectively. In the following we assume propagation in the z direction. Therefore we write $-j\sqrt{\varepsilon_{re}}$ for $\partial/\partial\overline{z}$. ε_{re} is the effective dielectric constant.

For the solution of the wave (1) and for the determination of the field components, a discretization in φ direction is performed [4]. As stated there, in principle, the analysis is the same as in Cartesian coordinates. Therefore, all that is known for the discretization in cartesian coordinates can be used here for the φ direction. In Fig. 1 two different possibilities are shown. To save memory and computational effort, absorbing boundary conditions (ABC) are suitable (a). If the whole cross section is of interest, periodic boundary conditions (PBC)

0018–9480/95$04.00 © 1995 IEEE

have to be used, which, in the most general case, are described in [1]. In the case of symmetry, or if the structure is only a part of the whole circle [4], Dirichlet and Neumann boundary conditions are suitable. For the discretization the following descriptions and definitions are used

$$E_z \rightarrow \boldsymbol{E}_z \tag{3}$$

$$h_\varphi \frac{\partial E_z}{\partial \varphi} \rightarrow \boldsymbol{D}_e \boldsymbol{E}_z \tag{4}$$

$$h_\varphi^2 \frac{\partial^2 E_z}{\partial \varphi^2} \rightarrow \boldsymbol{D}_h \boldsymbol{D}_e \boldsymbol{E}_z \tag{5}$$

$$\boldsymbol{\delta}_e = \boldsymbol{T}_h^{-1} \boldsymbol{D}_e \boldsymbol{T}_e \tag{6}$$

$$\boldsymbol{T}_e^{-1}(\boldsymbol{D}_h \boldsymbol{D}_e)\boldsymbol{T}_e = -\boldsymbol{\lambda}_e^2. \tag{7}$$

The discretization for H_z is dual. All subscripts e have to be changed in h and vice versa. h_φ is the (angular) discretization distance in the φ direction. $\boldsymbol{D}_e$ and $\boldsymbol{D}_h$ are the difference operators for the first order differential quotients. We obtain in the case of Neumann and/or Dirichlet conditions ([1], p. 386)

$$\boldsymbol{D}_h = -\boldsymbol{D}_e^t \quad \boldsymbol{T}_e^{-1} = \boldsymbol{T}_e^t \quad \boldsymbol{T}_h^{-1} = \boldsymbol{T}_h^t \tag{8}$$

in the case of periodic boundary conditions ([1], p. 443)

$$\boldsymbol{D}_h = -\boldsymbol{D}_e^{*t} \quad \boldsymbol{T}_e^{-1} = \boldsymbol{T}_e^{*t} \quad \boldsymbol{T}_h^{-1} = \boldsymbol{T}_h^{*t} \tag{9}$$

for the case of ABC's [13] [6]

$$\boldsymbol{D}_e = \boldsymbol{D}_a, \quad \boldsymbol{D}_h = -\boldsymbol{D}^t \quad \text{or} \quad \boldsymbol{D}_h = \boldsymbol{D}_a, \quad \boldsymbol{D}_e = -\boldsymbol{D}^t \tag{10}$$

$\boldsymbol{D}$ corresponds to $\boldsymbol{D}_a$. We get this operator from $\boldsymbol{D}_a$ by setting the parameters $a = 1$ and $b = c = 0$ [6] Furthermore, we have

$$\boldsymbol{\delta}_e \boldsymbol{\delta}_h = -\boldsymbol{\lambda}_h^2 \quad \boldsymbol{\delta}_h \boldsymbol{\delta}_e = -\boldsymbol{\lambda}_e^2 \tag{11}$$

$$\overline{\boldsymbol{\lambda}}^2 = h_\varphi^{-2} \boldsymbol{\lambda}^2 \quad \tilde{\boldsymbol{\delta}} = h_\varphi^{-1} \sqrt{\varepsilon_{re}}\boldsymbol{\delta} = \sqrt{\varepsilon_{re}}\tilde{\boldsymbol{\delta}}. \tag{12}$$

The discretization of the wave equation results in

$$t\frac{d}{dt}\left(t\frac{d\overline{\boldsymbol{F}}_z}{dt}\right) + (t^2\boldsymbol{I} - \overline{\boldsymbol{\lambda}}^2)\overline{\boldsymbol{F}}_z = \boldsymbol{0} \tag{13}$$

with $t = \sqrt{\varepsilon_d}\overline{\rho}$. $\overline{\boldsymbol{\lambda}}^2$ has the subscript $e(h)$ for $\boldsymbol{F}_z = \boldsymbol{E}_z(\tilde{\boldsymbol{H}}_z)$. The bars above the field quantities indicate that the quantities are transformed according to

$$\boldsymbol{E}_z = \boldsymbol{T}_e \overline{\boldsymbol{E}}_z \quad \tilde{\boldsymbol{H}}_z = \boldsymbol{T}_h \overline{\boldsymbol{H}}_z. \tag{14}$$

The general solution for the kth component is [4]

$$\overline{F}_{z_k} = J_{\overline{\lambda}_k}(t)A_k + Y_{\overline{\lambda}_k}(t)B_k. \tag{15}$$

In the following we use $\boldsymbol{\nu} = \overline{\boldsymbol{\lambda}}$ instead of $\overline{\boldsymbol{\lambda}}$. The boldface subscript $\boldsymbol{\nu}$, on both the cylinder functions $\mathcal{C}$ and functions constructed from them, means that, e.g., $\mathcal{C}_{\boldsymbol{\nu}}$ is a diagonal matrix and consists of the elements $\mathcal{C}_{\nu_k}$. The discretized transverse field components are obtained from E_z and H_z as follows

$$\varepsilon_d \begin{bmatrix} \overline{\rho}\overline{\boldsymbol{E}}_\varphi \\ \overline{\rho}\overline{\boldsymbol{H}}_\varphi \end{bmatrix} = j \begin{bmatrix} -\tilde{\boldsymbol{\delta}}_e & D_t \boldsymbol{I}_h \\ -\varepsilon_r D_t \boldsymbol{I}_e & -\tilde{\boldsymbol{\delta}}_h \end{bmatrix} \begin{bmatrix} \overline{\boldsymbol{E}}_z \\ \overline{\boldsymbol{H}}_z \end{bmatrix} \tag{16}$$

$$\varepsilon_d \begin{bmatrix} \overline{\rho}\overline{\boldsymbol{E}}_\rho \\ \overline{\rho}\overline{\boldsymbol{H}}_\rho \end{bmatrix} = -j \begin{bmatrix} \sqrt{\varepsilon_{re}}\boldsymbol{I}_e D_t & \boldsymbol{\delta}_h \\ -\varepsilon_r \boldsymbol{\delta}_e & \sqrt{\varepsilon_{re}}\boldsymbol{I}_h D_t \end{bmatrix} \begin{bmatrix} \overline{\boldsymbol{E}}_z \\ \overline{\boldsymbol{H}}_z \end{bmatrix} \tag{17}$$

where $\varepsilon_d = \varepsilon_r - \varepsilon_{re}$ and $D_t = t(d/dt)$. The quantities $\boldsymbol{E}_\rho, \tilde{\boldsymbol{H}}_\varphi$ are transformed with $\boldsymbol{T}_e$ and $\tilde{\boldsymbol{H}}_\rho, \boldsymbol{E}_\rho$ with $\boldsymbol{T}_h$, respectively. $\boldsymbol{I}$ is the identity matrix.

C. Fields on the Interfaces A and B

From the general solution in (15) we have for the interfaces A and B of a layer in matrix form

$$\begin{bmatrix} \overline{F}_{zA} \\ \overline{F}_{zB} \end{bmatrix} = \begin{bmatrix} J_{\boldsymbol{\nu}}(t_A) & Y_{\boldsymbol{\nu}}(t_A) \\ J_{\boldsymbol{\nu}}(t_B) & Y_{\boldsymbol{\nu}}(t_B) \end{bmatrix} \begin{bmatrix} \boldsymbol{A} \\ \boldsymbol{B} \end{bmatrix}. \tag{18}$$

After differentiating (18) with respect to the argument and introducing the vector of the coefficients from (18), we obtain

$$t\frac{d}{dt}\begin{bmatrix} \overline{\boldsymbol{F}}_{z_A} \\ \overline{\boldsymbol{F}}_{z_B} \end{bmatrix} = \hat{p}_{\boldsymbol{\nu}}^{-1} \begin{bmatrix} \overline{r}_{\boldsymbol{\nu}} & \frac{2}{\pi}\boldsymbol{I} \\ -\frac{2}{\pi}\boldsymbol{I} & \overline{q}_{\boldsymbol{\nu}} \end{bmatrix} \begin{bmatrix} \overline{\boldsymbol{F}}_{z_A} \\ \overline{\boldsymbol{F}}_{z_B} \end{bmatrix} \tag{19}$$

The hat ($\hat{}$) above a quantity here and in the following is used to indicate that the quantity is a blocdiagonal matrix constructed from two matrices without a hat, e.g.,

$$\hat{p}_{\boldsymbol{\nu}} = \mathrm{Diag}(p_{\boldsymbol{\nu}}, p_{\boldsymbol{\nu}}). \tag{20}$$

Here, as in (19), we have used the cross products according to the definitions 9.1.32 in [11] which we normalize

$$\overline{r}_{\boldsymbol{\nu}} = t_A r_{\boldsymbol{\nu}} \quad \overline{q}_{\boldsymbol{\nu}} = t_B q_{\boldsymbol{\nu}} \quad \overline{s}_{\boldsymbol{\nu}} = t_A t_B s_{\boldsymbol{\nu}}. \tag{21}$$

Analogous to (26) in [1], instead of (16) we can now write

$$\varepsilon_d \begin{bmatrix} \overline{\rho}_{AB}\overline{\boldsymbol{E}}_{\varphi AB} \\ \overline{\rho}_{AB}\overline{\boldsymbol{H}}_{\varphi AB} \end{bmatrix} = \begin{bmatrix} \hat{\tilde{\boldsymbol{\delta}}}_e & \boldsymbol{\Gamma}_h \\ \varepsilon_r \boldsymbol{\Gamma}_e & -\hat{\tilde{\boldsymbol{\delta}}}_h \end{bmatrix} \begin{bmatrix} -j\overline{\boldsymbol{E}}_{zAB} \\ -j\overline{\boldsymbol{H}}_{zAB} \end{bmatrix} \tag{22}$$

$$\overline{\boldsymbol{F}}_{zAB} = [\overline{\boldsymbol{F}}_{zA}^t, \overline{\boldsymbol{F}}_{zB}^t]^t \tag{23}$$

$$\overline{\rho}_{AB}\overline{\boldsymbol{F}}_{\varphi AB} = [\overline{\rho}_A \overline{\boldsymbol{F}}_{\varphi A}^t, \overline{\rho}_B \overline{\boldsymbol{F}}_{\varphi B}^t]^t \tag{24}$$

where the $\boldsymbol{\Gamma}$ and $\boldsymbol{\Gamma}^{-1}$ matrices are given by

$$\boldsymbol{\Gamma} = \hat{p}_{\boldsymbol{\nu}}^{-1} \begin{bmatrix} \overline{r}_{\boldsymbol{\nu}} & \frac{2}{\pi}\boldsymbol{I} \\ -\frac{2}{\pi}\boldsymbol{I} & \overline{q}_{\boldsymbol{\nu}} \end{bmatrix} \quad \boldsymbol{\Gamma}^{-1} = \hat{s}_{\boldsymbol{\nu}}^{-1} \begin{bmatrix} \overline{q}_{\boldsymbol{\nu}} & -\frac{2}{\pi}\boldsymbol{I} \\ \frac{2}{\pi}\boldsymbol{I} & \overline{r}_{\boldsymbol{\nu}} \end{bmatrix}. \tag{25}$$

The inversion of the matrix $\boldsymbol{\Gamma}$ was obtained with 9.1.34 in [11]. Therefore, (22) takes the following form

$$\begin{bmatrix} j\overline{\boldsymbol{H}}_{zAB} \\ \overline{\rho}_{AB}\overline{\boldsymbol{H}}_{\varphi AB} \end{bmatrix} = \begin{bmatrix} \varepsilon_d \boldsymbol{\Gamma}_h^{-1} & \boldsymbol{\Gamma}_h^{-1}\hat{\tilde{\boldsymbol{\delta}}}_e \\ -\boldsymbol{\Gamma}_e^{-1}\hat{\tilde{\boldsymbol{\delta}}}_h & \boldsymbol{\Gamma}_E \end{bmatrix} \begin{bmatrix} \overline{\rho}_{AB}\overline{\boldsymbol{E}}_{\varphi AB} \\ j\overline{\boldsymbol{E}}_{zAB} \end{bmatrix} \tag{26}$$

$$\begin{aligned} \boldsymbol{\Gamma}_E &= \begin{bmatrix} \gamma_{E_1} & -\boldsymbol{\alpha}_E \\ \boldsymbol{\alpha}_E & \gamma_{E_2} \end{bmatrix} \\ \gamma_{E_1} &= \varepsilon_d^{-1}(-\varepsilon_r \overline{r}_{\boldsymbol{\nu}_e} p_{\boldsymbol{\nu}_e}^{-1} + \varepsilon_{re}\overline{q}_{\boldsymbol{\nu}_e}\overline{s}_{\boldsymbol{\nu}_e}^{-1}\overline{\boldsymbol{\lambda}}_e^2) \\ \gamma_{E_2} &= \varepsilon_d^{-1} \\ \boldsymbol{\alpha}_E &= \frac{2}{\pi}\varepsilon_d^{-1}(\varepsilon_r p_{\boldsymbol{\nu}_e}^{-1} + \varepsilon_{re}\overline{s}_{\boldsymbol{\nu}_e}^{-1}\overline{\boldsymbol{\lambda}}_e^2) \end{aligned} \tag{27}$$

γ_{E_2} is obtained from γ_{E_1} by replacing $\overline{r}_{\boldsymbol{\nu}_e}$ by $\overline{q}_{\boldsymbol{\nu}_e}$ and vice versa. For this formulation we have used the relations $\boldsymbol{\delta}_e \boldsymbol{u}_e = \boldsymbol{u}_h \boldsymbol{\delta}_e$ and $\boldsymbol{\delta}_h \boldsymbol{u}_h = \boldsymbol{u}_e \boldsymbol{\delta}_h$ [1], where, $\boldsymbol{u}_{e,h}$ is one of the diagonal matrices, e.g., $\overline{r}_{\boldsymbol{\nu}}, p_{\boldsymbol{\nu}}, \overline{q}_{\boldsymbol{\nu}}, \overline{s}_{\boldsymbol{\nu}}$.

The last step in our derivation is the rewriting of (26). With the following definitions

$$\overline{\boldsymbol{H}}_{A,B} = [j\overline{\boldsymbol{H}}_{zA,B}^t, \overline{\rho}_{A,B}\overline{\boldsymbol{H}}_{\varphi A,B}^t]^t \tag{28}$$

$$\overline{\boldsymbol{E}}_{A,B} = [\overline{\rho}_{A,B}\overline{\boldsymbol{E}}_{\varphi A,B}^t, j\overline{\boldsymbol{E}}_{zA,B}^t]^t \tag{29}$$

we obtain

$$\begin{bmatrix} \overline{\boldsymbol{H}}_A \\ \overline{\boldsymbol{H}}_B \end{bmatrix} = \begin{bmatrix} \overline{\boldsymbol{y}}_{1A} & \overline{\boldsymbol{y}}_2 \\ \overline{\boldsymbol{y}}_2 & \overline{\boldsymbol{y}}_{1B} \end{bmatrix} \begin{bmatrix} \overline{\boldsymbol{E}}_A \\ -\overline{\boldsymbol{E}}_B \end{bmatrix} \tag{30}$$

$$\overline{\boldsymbol{y}}_{1A} = \begin{bmatrix} \varepsilon_d \overline{q}_{\boldsymbol{\nu}_h}\overline{s}_{\boldsymbol{\nu}_h}^{-1} & \overline{q}_{\boldsymbol{\nu}_h}\overline{s}_{\boldsymbol{\nu}_h}^{-1}\tilde{\boldsymbol{\delta}}_e \\ -\tilde{\boldsymbol{\delta}}_h \overline{q}_{\boldsymbol{\nu}_h}\overline{s}_{\boldsymbol{\nu}_h}^{-1} & \gamma_{E_1} \end{bmatrix} \tag{31}$$

$$\overline{\boldsymbol{y}}_2 = \begin{bmatrix} \frac{2}{\pi}\varepsilon_d \overline{s}_{\boldsymbol{\nu}_h}^{-1} & \frac{2}{\pi}\overline{s}_{\boldsymbol{\nu}_h}^{-1}\tilde{\boldsymbol{\delta}}_e \\ -\frac{2}{\pi}\tilde{\boldsymbol{\delta}}_h \overline{s}_{\boldsymbol{\nu}_h}^{-1} & \boldsymbol{\alpha}_E \end{bmatrix} \tag{32}$$

$\overline{\boldsymbol{y}}_{1B}$ is obtained from $\overline{\boldsymbol{y}}_{1A}$ by replacing γ_{E_1} by $-\gamma_{E_2}$ and $\overline{q}_{\boldsymbol{\nu}_h}$ by $-\overline{r}_{\boldsymbol{\nu}_h}$. With $\overline{\boldsymbol{H}}_A = \overline{\boldsymbol{Y}}_t^{(k-1)}\overline{\boldsymbol{E}}_A$ and $\overline{\boldsymbol{H}}_B = \overline{\boldsymbol{Y}}_t^{(k)}\overline{\boldsymbol{E}}_B$, the following recursion formula is obtained

$$\boldsymbol{Y}_t^{(k)} = \overline{\boldsymbol{y}}_2(\overline{\boldsymbol{y}}_{1A} - \overline{\boldsymbol{Y}}_t^{(k-1)})^{-1}\overline{\boldsymbol{y}}_2 - \overline{\boldsymbol{y}}_{1B} \tag{33}$$

for the transfer of the admittance in the outward direction. With $\overline{\boldsymbol{H}}_B = -\overline{\boldsymbol{Y}}_t^{(l-1)}\overline{\boldsymbol{E}}_B$ and $\overline{\boldsymbol{H}}_A = -\overline{\boldsymbol{Y}}_t^{(l)}\overline{\boldsymbol{E}}_A$, the transfer from an outer to an inner boundary is obtained

$$\overline{\boldsymbol{Y}}_t^{(l)} = \overline{\boldsymbol{y}}_2(\overline{\boldsymbol{y}}_{1B} - \overline{\boldsymbol{Y}}_t^{(l-1)})^{-1}\overline{\boldsymbol{y}}_2 - \overline{\boldsymbol{y}}_{1A}. \tag{34}$$

An equation analogous to (26) in [1] reads

$$\begin{bmatrix}\overline{\boldsymbol{E}}_B\\ \overline{\boldsymbol{H}}_B\end{bmatrix} = \begin{bmatrix}\overline{\boldsymbol{V}}_1 & \overline{\boldsymbol{Z}}\\ \overline{\boldsymbol{Y}} & \overline{\boldsymbol{V}}_2\end{bmatrix}\begin{bmatrix}\overline{\boldsymbol{E}}_A\\ \overline{\boldsymbol{H}}_A\end{bmatrix} \tag{35}$$

$$\overline{\boldsymbol{V}}_1 = \overline{\boldsymbol{y}}_2^{-1}\overline{\boldsymbol{y}}_{1A} \quad \overline{\boldsymbol{V}}_2 = \overline{\boldsymbol{y}}_{1B}\overline{\boldsymbol{y}}_2^{-1}$$
$$\overline{\boldsymbol{Z}} = -\overline{\boldsymbol{y}}_2^{-1} \quad \overline{\boldsymbol{Y}} = \overline{\boldsymbol{y}}_2 - \overline{\boldsymbol{y}}_{1B}\overline{\boldsymbol{y}}_2^{-1}\overline{\boldsymbol{y}}_{1A}. \tag{36}$$

Equation (35) is a generalized transfer equation. The transfer equation for a number of layers is obtained by multiplication of the matrices for the single layers.

The usage of the derived formulas is analogous to that for Cartesian coordinates [1], e.g., the system reduction in the spatial domain because of the metallic conductors (strips) is identical. Formulas for the power transfer necessary for the impedances are given in the Appendix.

III. Extensions

The summarized procedure for analysis can easily be extended for finite metallization thickness, two-dimensional discretization, lossy material, or higher order difference operator approximation. As shown in Section II, the discretization in azimuthal direction does not differ from the discretization in Cartesian coordinates. Therefore all what is known for the nonequidistant discretization in Cartesian coordinates [16] can be used here in the same way. The higher order approximation derived in [15] can be used to improve the convergence behavior. To take into account the finite metallization thickness, the formalism given in [1] and [14] can be directly used. It should be remembered that we have two different matrices $\overline{\boldsymbol{y}}_{1A}$ and $\overline{\boldsymbol{y}}_{1B}$ instead of a single matrix $\overline{\boldsymbol{y}}_1$.

If the structure is not homogeneous in the z direction, then a discretization for this coordinate is also necessary. The z-coordinate, however, is a Cartesian coordinate, and therefore the discretization in this direction is completely analogous to the procedures given in [1], [12], and [6].

IV. Conclusion

With the general formulas presented here, the analysis of multilayered cylindrical structures can be performed using the MoL. Because the discretization procedure in principle was verified in [4] no special numerical results are given.

Appendix
Calculation of the Power Transfer for the Characteristic Impedance

In waveguides allowing hybrid waves propagation, characteristic impedances are defined by means of the power transfer P [1]. The power transfer P is determined as the integral of the Poynting vector over the waveguide cross section F. For propagation in the z direction,

$$P = \mathrm{Re}\left\{\iint_F [e_\rho h_\varphi^* - e_\varphi h_\rho^*]\rho\, d\varphi\, d\rho\right\}. \tag{A.1}$$

The power transfer must be calculated separately for each layer of the circular structure and then summed over all layers. For the layer between ρ_A and ρ_B in Fig. 1 we obtain using the discretized fields (approximating the integral with respect to φ by means of the rectangular or trapezoidal rule)

$$P_d = \mathrm{Re}\left\{\frac{h}{k_0^2\varepsilon_d}\int_{t_A}^{t_B}[t\boldsymbol{H}_\varphi^{*t}\boldsymbol{E}_\rho - t\boldsymbol{H}_\rho^{*t}\boldsymbol{E}_\varphi]\,dt\right\}. \tag{A.2}$$

Instead of using the field components in the spatial domain, the field components in the transformed domain can be used to an advantage, because, e.g.,

$$\boldsymbol{H}_\varphi^{*t}\boldsymbol{E}_\rho = \boldsymbol{H}_\varphi^{*t}\boldsymbol{T}_e\overline{\boldsymbol{E}}_\rho = (\boldsymbol{T}_e^{*t}\boldsymbol{H}_\varphi)^{*t}\overline{\boldsymbol{E}}_\rho = \overline{\boldsymbol{H}}_\varphi^{*t}\overline{\boldsymbol{E}}_\rho. \tag{A.3}$$

With

$$\overline{\boldsymbol{F}} = \begin{bmatrix}J_{\boldsymbol{\nu}}(t)\\ Y_{\boldsymbol{\nu}}(t)\end{bmatrix}^t \hat{p}_{\boldsymbol{\nu}}^{-1}\begin{bmatrix}Y_{\boldsymbol{\nu}}(t_B) & -Y_{\boldsymbol{\nu}}(t_A)\\ -J_{\boldsymbol{\nu}}(t_B) & J_{\boldsymbol{\nu}}(t_A)\end{bmatrix}\begin{bmatrix}\overline{\boldsymbol{F}}_A\\ \overline{\boldsymbol{F}}_B\end{bmatrix} \tag{A.4}$$

where $\overline{F} = \overline{\boldsymbol{E}}_\rho$ or $\overline{F} = \overline{\boldsymbol{H}}_\varphi$ and with the solutions of the following integrals

$$\int_{t_A}^{t_B}\begin{bmatrix}tJ_{\boldsymbol{\nu}}^2(t) & tJ_{\boldsymbol{\nu}}(t)Y_{\boldsymbol{\nu}}(t)\\ tJ_{\boldsymbol{\nu}}(t)Y_{\boldsymbol{\nu}}(t) & tY_{\boldsymbol{\nu}}^2(t)\end{bmatrix}dt = \begin{bmatrix}a_{\boldsymbol{\nu}} & b_{\boldsymbol{\nu}}\\ b_{\boldsymbol{\nu}} & c_{\boldsymbol{\nu}}\end{bmatrix} \tag{A.5}$$

we obtain the final result for the first part of (A.2)

$$\int_{t_A}^{t_B} t\boldsymbol{H}_\varphi^{*t}\boldsymbol{E}_\rho dt = \begin{bmatrix}\overline{\boldsymbol{H}}_{\varphi A}\\ \overline{\boldsymbol{H}}_{\varphi B}\end{bmatrix}^{*t}\begin{bmatrix}\boldsymbol{g}_B & \boldsymbol{g}_2\\ \boldsymbol{g}_2 & \boldsymbol{g}_A\end{bmatrix}\begin{bmatrix}\overline{\boldsymbol{E}}_{\rho A}\\ \overline{\boldsymbol{E}}_{\rho B}\end{bmatrix} \tag{A.6}$$

with $(C = A \text{ or } B)$

$$\boldsymbol{g}_C = [a_{\boldsymbol{\nu}}Y_{\boldsymbol{\nu}}^2(t_C) + c_{\boldsymbol{\nu}}J_{\boldsymbol{\nu}}^2(t_C) - 2b_{\boldsymbol{\nu}}J_{\boldsymbol{\nu}}(t_C)Y_{\boldsymbol{\nu}}(t_C)]p_{\boldsymbol{\nu}}^{-2}$$
$$\boldsymbol{g}_2 = (-a_{\boldsymbol{\nu}}Y_{\boldsymbol{\nu}}(t_A)Y_{\boldsymbol{\nu}}(t_B) - c_{\boldsymbol{\nu}}J_{\boldsymbol{\nu}}(t_A)J_{\boldsymbol{\nu}}(t_B))p_{\boldsymbol{\nu}}^{-2}$$
$$+ b_{\boldsymbol{\nu}}(J_{\boldsymbol{\nu}}(t_A)Y_{\boldsymbol{\nu}}(t_B) + J_{\boldsymbol{\nu}}(t_B)Y_{\boldsymbol{\nu}}(t_A))p_{\boldsymbol{\nu}}^{-2}. \tag{A.7}$$

The subscript $\boldsymbol{\nu}$ must be marked with a subscript e. A corresponding result is also obtained for the second term in (A.2), but $\boldsymbol{\nu}$ must then be marked with a subscript h.

Acknowledgment

The author would like to thank W. Pascher for discussions and helpful comments.

References

[1] R. Pregla and W. Pascher, "The method of lines," T. Itoh, Ed.,, in *Numerical Techniques for Microwave and Millimeter Wave Passive Structures.* New York: Wiley, 1989, pp. 381–446.

[2] U. Rogge and R. Pregla, "The method of lines for the analysis of strip-loaded optical waveguides," *J. Lightwave Technol.*, vol. 11, pp. 2015–2020, Dec. 1993.

[3] U. Rogge and R. Pregla, "The method of lines for the analysis of strip loaded optical waveguides," *J. Opt. Soc. Am. B*, vol. 8, no. 2, pp. 459–463, 1991.

[4] Y. Xu, "Application of the method of lines to solve problems in the cylindrical coordinates," *Microwave Opt. Technol. Lett.*, vol. 1, no. 5, pp. 173–175, July 1988.

[5] Y.-J. He and S.-F. Li, "Analysis of arbitrary cross-section microstrip using the method of lines," *IEEE Trans. Microwave Theory Tech.*, vol. 42, no. 1, pp. 162–164, Jan. 1994.

[6] R. Pregla and L. Vietzorreck, "Calculation of input impedances of planar antennas with the method of lines," in *Proc. PIERS 1994.* The Netherlands: Noordwijk, July 1994, on CD-ROM.

[7] R. Pregla, "New approach for the analysis of cylindrical antennas by the method of lines," *Electron. Lett.*, vol. 30, no. 8, pp. 614–615, Apr. 1994.

[8] W. Pascher and R. Pregla, "Vectorial analysis of bends in optical strip waveguides by the method of lines," *Radio Sci.*, vol. 28, no. 6, pp. 1229–1233, 1993.

[9] ——, "Analysis of curved optical waveguides by the vectorial method of lines," in *Proc. Int. Conf. Integrated Optics Optical Fiber Commun.*, Paris, 1991, pp. 237–240.

[10] R. Pregla, "Method of lines for the analysis of multilayered gyrotropic waveguide structures," *IEE Proc. H,* vol. 140, no. 3, pp. 183–192, June 1993.
[11] M. Abramowitz and I. A. Stegun, *Handbook of Mathematical Functions with Formulas, Graphs, and Mathematical Tables.* New York: Dover.
[12] W. Pascher, "Full wave analysis of discontinuities in planar waveguides by the method of lines," in *Proc. URSI Int. Symp. Electromagnetic Theory,* Stockholm, Sweden, Aug. 1989, pp. 446–448.
[13] A. Dreher and R. Pregla, "Full-wave analysis of radiating planar resonators with the method of lines," *IEEE Trans. Microwave Theory Tech.*, vol. 41, no. 8, pp. 1363–1368, Aug. 1993.
[14] F. J. Schmückle and R. Pregla, "The method of lines for the analysis of planar waveguides with finite metallization thickness," *IEEE Trans. Microwave Theory Tech.*, vol. 39, no. 1, pp. 107–111, Jan. 1991.
[15] R. Pregla, "Higher order approximation for the difference operators in the method of lines," *IEEE Microwave Guided Wave Lett.*, vol. 5, no. 2, Feb. 1995.
[16] H. Diestel and S. B. Worm, "Analysis of hybrid field problems by the method of lines with nonequidistant discretization," *IEEE Trans. Microwave Theory Tech.*, vol. 32 , no. 6, pp. 633–638, June 1984.

Magnetic Frequency-Tunable Millimeter-Wave Filter Design Using Metallic Thin Films

Hoton How, Ta-Ming Fang, and Carmine Vittoria

***Abstract*— Frequency tunable millimeter wave filters are considered to be fabricated using metallic ferromagnetic thin films. Whereas conventional filters which include insulating ferrite materials utilize the phenomenon of ferromagnetic resonance (FMR), our design incorporates the phenomenon of ferromagnetic anti-resonance (FMAR). Our calculations indicate that in comparing the characteristics of the two types of filters the filter utilizing magnetic metal films is superior in terms of insertion loss and integrability with other planar millimeter wave devices. Design of band-pass filter can be realized in which the transmission frequency occurs at FMAR frequency with a frequency bandwidth equal to the FMAR linewidth.**

I. Introduction

In the past microwave/millimeter wave filters were inevitably designed in terms of varying the capacitive or inductive loading of the resonators. For the former case varactors are commonly used in which the frequency tuning range of the filter can be only a few percent of the transmission frequency [1]. For the latter case ferrite insulators are used which are usually in the form of polished spheres of single crystal yttrium iron garnet (YIG). The ferrite spheres are biased by a magnetic field and the transmission frequency is designed at ferromagnetic resonance (FMR) [2]. Both designs involving varactors and ferrite insulators are limited to relatively low-power applications.

We consider in this paper for the first time a new design in which metallic magnetic films are used instead of ferrites in order to improve the band-pass characteristics. Whereas conventional insulating ferrite materials utilize the phemomenon of ferromagnetic resonance (FMR), the use of magnetic metal films utilizes the phenomenon of ferromagnetic anti-resonance (FMAR). Normally metals more than a few μ thick are opaque to microwave radiation. However, it was predicted by Kaganov [3] (1959) and discovered by Heinrich and Meshcheryakov [4] (1969) that a ferromagnetic metal becomes relatively transparent to microwave radiation over a limit range of applied magnetic fields near the field strength corresponding to FMAR. At FMAR the effective permeability of the metal film is very small and, hence, the resultant microwave skin depth becomes anomalously large. Additional work on this subject may be found in [5]–[7].

Our filter design involves the fabrication of a composite microstrip line in which a thin magnetic metal film is inserted in the substrate layer of the microstrip line, which is connected to and lies parallel to the ground plane. The characteristic impedance of the microstrip line in the absence of the metal film is 50 Ω. A dc magnetic field is applied normal to the film plane. When the magnetic film is biased away from FMAR the magnetic metal film interferes strongly with wave propagation. The characteristic impedance of the line appears to be much smaller than 50 Ω. The signal is reflected when biased off-FMAR due to impedance mismatch. However, for biasing field at FMAR the skin depth within the magnetic metal becomes substantially greater than the film thickness. Consequently, at FMAR the impedance of the line changes to 50 Ω which matches the input signal feeder line. The band-pass transmission bandwidth is consequently the FMAR linewidth [5]–[7]. We have calculated the transmission properties of the filter based on the use of permalloy thin films. The calculations show the following characteristics: insertion loss is less than 0.2 dB, isolation larger than 10 dB, and frequency tunability extends from 30 to 120 GHz.

FMAR occurs for frequencies somewhat above FMR. At FMAR the rf magnetic moment, $\boldsymbol{m}$, is out-of-phase with the driving field, $\boldsymbol{h}$, so that [5]–[7]

$$\boldsymbol{b} = \boldsymbol{h} + 4\pi\boldsymbol{m} = 0. \tag{1}$$

For this condition the dynamic permeability, μ, is very small (limited by the value of magnetic relaxation) and the effective skin depth is large, being limited only by the magnetic damping. The condition of (1) combined with the magnetic equation of motion

$$\boldsymbol{M} = \gamma \boldsymbol{M} \times \boldsymbol{H} \tag{2}$$

where

$$\boldsymbol{H} = \boldsymbol{H}_0 + \boldsymbol{h}$$

readily leads to the condition for FMAR

$$\omega/\gamma = B_0 = H_{\text{in}} + 4\pi M_s \tag{3}$$

where H_{in} is the static internal magnetic field, γ the gyromagnetic ratio, and $4\pi M_s$ the saturation magnetization.

At FMAR the metal film is characterized by a small permeability value which results in very large skin depth when the metal film is exposed to rf excitations [5]–[7]. Therefore, the metal film appears to be transparent to the microwave millimeter wave transmission when it is biased at FMAR. The frequency bandwidth of transmission is roughly equal to the linewidth at FMAR [3]

$$\Delta H_{\text{FMAR}} = 0.3(4\pi M_s)[(\delta_s/d)(\Delta H/M_s)^{3/2}]^{1/2} \tag{4}$$

where d is the thickness of the metal film, δ_s the classical skin depth

$$\delta_s = c/(2\pi\sigma\omega)^{1/2}$$

c the speed of light in vacuum, σ the conductivity of the metal film, and ΔH is the linewidth at FMR given by

$$\Delta H = 2(\lambda/\gamma)(\omega/\gamma M_s). \tag{5}$$

Here λ denotes the Landau–Lifshitz damping parameter [6].

Manuscript received February 16, 1994; revised January 20, 1995. This work was supported by the Strategic Defense Initiative Office and managed and executed by the Defense Nuclear Agency (Contract DNA001-94-C-0076).

H. How and T.-M. Fang are with the Massachusetts Technological Laboratory, Belmont, MA 02178 USA.
C. Vittoria is with Northeastern University, Boston, MA 02115 USA.

IEEE Log Number 9412030.

0018–9480/95$04.00 © 1995 IEEE